Excitons as intermediate states in spin-flip Raman scattering of electrons bound to donors in $Cd_{1-x}Mn_xTe$ epilayers

M. Hirsch, R. Meyer, and A. Waag
Physikalisches Institut der Universität Würzburg, 97074 Würzburg, Federal Republic of Germany
(Received 27 January 1993)

The resonance behavior of the spin-flip Raman scattering in semimagnetic $Cd_{1-x}Mn_xTe$ epilayers has been used to investigate the scattering process itself as well as to identify the state of the carrier that changes its spin. The characteristic variation of the Stokes shift with magnetic field, a magnetic polaron effect for vanishing magnetic field, and the independence of the scattering efficiency of laser power indicate that a donor-bound electron changes its spin orientation. According to magnetic dipole selection rules of electrons for the spin-flip scattering, the Raman signal shows resonances with excitonic transitions involving the $m_j = \pm\frac{1}{2}$ hole states as they can be characterized by luminescence and photoluminescence excitation spectroscopy. The pronounced resonance behavior allows a very accurate comparison of the resonance energy of the spin-flip Raman scattering with the energetic position of the corresponding free exciton peak in the photoluminescence excitation spectrum. We therefrom conclude that a donor-bound exciton plays the role of the intermediate state in this scattering process.

I. INTRODUCTION

Semimagnetic semiconductors like $Cd_{1-x}Mn_xTe$, where the group-IIb element is (partially) replaced by paramagnetic ions (e.g., Mn^{2+}) combine an energy gap in near infrared or the visible with unusually large spin splittings of valence and conduction bands.[1] The latter is due to the strong exchange interaction between the localized *3d* states of the Mn^{2+} and the extended states at the band edge. Spin-flip Raman scattering (SFRS) has been widely used to study the spin splittings of both bound[2–7] and free[8,9] electrons in the Mn^{2+} containing Cd and Zn chalcogenides as well as in some Fe^{2+} containing Cd chalcogenides.[10–14]

Antisymmetric components of the Raman tensor, where the polarizations of incident and scattered photon $\mathbf{e}_I$ and $\mathbf{e}_S$ have to be perpendicular to each other, are characteristic for light scattering on magnetic excitations. If one of the two polarizations is parallel to the magnetic field, the net spin of the radiation field is changed leaving the crystal in a spin state altered by $\triangle m_j = \pm 1$. In this case of SFRS the observed Raman shift displays the corresponding spin splitting. If $\mathbf{e}_I$ and $\mathbf{e}_S$ both are perpendicular to the direction $\mathbf{e}_B$ of the magnetic field [i.e., $(\mathbf{e}_I \times \mathbf{e}_S) \cdot \mathbf{e}_B \neq 0$], the photon can couple to fluctuations of the spin density without changing the net spin of the crystal.[15] In this scattering geometry a second allowed process is the exchange of a net spin of $\triangle m_j = \pm 2$ between the radiation field and the crystal. Although a lot of work has been done on the resonance behavior of Raman scattering on spin density excitations, only a few investigations about the resonance behavior of SFRS exist. This is due to the fact that in nonmagnetic semiconductor bulk crystals spin splittings, large enough to allow a reasonable measurement of the resonance behavior, are found only in narrow-gap materials.[16] For these materials, however, tunable lasers are not easily available, which cover the energy range of the fundamental gap.

For the Raman scattering on phonons it has been shown[17,18] that in semimagnetic semiconductors the large spin splitting of the excitonic transitions in a magnetic field results in well-separated Raman resonances. For Raman scattering on magnetic excitations so far the large spin splitting has been used to investigate the resonance behavior of SFRS on bound electrons in a prelimary study on $CdTe/Cd_{1-x}Mn_xTe$ quantum-well structures[19] as well as in *p*-type $Cd_{1-x}Mn_xTe$ bulk material.[20] The spin-flip Raman scattering on transitions in the Zeeman split ${}^6S_{5/2}$ ground state of the Mn^{2+} *3d* levels in $Cd_{1-x}Mn_xTe$ and the Raman scattering on the *3d* ground state of Fe^{2+} in $Cd_{1-x}Fe_xTe$ also display resonances with the excitonic transitions close to the fundamental band gap. Since we have discussed the corresponding scattering process elsewhere in preliminary form,[21,14] a more detailed presentation will follow. In the present paper we report on a study of Raman scattering by the spin of bound electrons emphasizing the resonance behavior of this process in undoped and *n*-type $Cd_{1-x}Mn_xTe$ epilayers grown by molecular-beam epitaxy (MBE). These resonances give detailed information on the intermediate states involved in the Raman-scattering process.

II. EXPERIMENTAL DETAILS

We investigated $Cd_{1-x}Mn_xTe$:In epilayers with Mn concentration ($0.01 \leq x \leq 0.21$) grown by photoassisted molecular-beam epitaxy (PAMBE), where during growth the surface was illuminated by an Ar^+ laser with the number of incident photons about 100 times larger than the number of incident particles. The PAMBE has proved to allow n-type doping with high carrier concentrations and increased mobilities because it helps to avoid self-compensation related to Cd vacancies which act as double acceptors.[22] Indium was used as substitutional dopant at unknown concentration. (001)-oriented CdTe or $Cd_{0.96}Zn_{0.04}Te$ wafers have been used as substrates, chosen to minimize the lattice mismatch to $\triangle a/a < 0.2\,\%$. As a $Cd_{0.96}Zn_{0.04}Te$ substrate is lattice matched to a $Cd_{0.885}Mn_{0.115}Te$ layer, the epilayers with a typical thickness of 1.5–7 μm are only weakly strained. Mn concentration was measured by the free exciton structures as they are displayed by photoluminescence excitation spectroscopy (PLE). Biaxial strain was determined by the light-hole–heavy-hole splitting of these excitons. For the Raman experiments the backscattering geometry has to be used due to the strong absorption of the excitonic transitions. The directions of the wave vectors of incident and scattered light therefore are parallel to the (001) growth direction. According to SFRS selection rules the magnetic field ($B < 7.5\,\mathrm{T}$) has to be perpendicular to the direction of light propagation, i.e., parallel to the surface. The direction of the magnetic field was chosen along the cubic (010) axis. One therefore expects SFRS in the $\bar{z}(\sigma,\pi)z$ and in the $\bar{z}(\pi,\sigma)z$ scattering geometry with $\pi \parallel \mathbf{B} \parallel (010)$ and $\sigma \parallel (100)$.

For excitation we used an Ar^+ laser pumped dye laser. Luminescence and scattered light were collected by $f/6.5$ optics and analyzed by a 0.5-m triple Raman spectrometer equipped with an optical multichannel analyzer. A slit width of 100 μm typically used for the experiments leads to an overall spectral resolution of 0.2 meV. To measure the resonance behavior of Raman scattering (or to measure PLE) the exciting beam of the dye laser was split to monitor the laser power while recording the spectrum. The intensity of the Raman signal (or in the case of PLE, the intensity of the luminescence signal) was measured as a function of laser energy and normalized respective to the exciting laser power. No attempt was made to correct the Raman resonance profiles for reflection at the sample surface and absorption in the epitaxial films.

According to mean-field theory the spin splitting of band-edge states in $Cd_{1-x}Mn_xTe$ is proportional to the averaged Mn *3d* spin orientation within the wave-function range of the carrier. Therefore, the Stokes shift of the SFRS signal displays a Brillouin-function-like behavior with varying magnetic field and is also a very sensitive probe of the Mn spin temperature. For our measurements the samples were immersed in liquid He ($T = 1.6-1.8\,\mathrm{K}$). To avoid local heating, a line focus was produced on the sample surface by a cylindrical lens leading to typical power densities smaller than 1 W cm^{-2}. An increase from still lower power densities to this value results in a small decrease in the observed Stokes shift of the spin-flip Raman excitation (of the order of 0.2 meV, i.e., < 1%). This corresponds to a laser-induced increase of the Mn spin temperature by 0.2 K.

III. EXPERIMENTAL RESULTS AND THEIR DISCUSSION

A. Raman excitation

In the following we will focus on a $Cd_{0.865}Mn_{0.135}Te$ epilayer with thickness 1.6 μm. The investigations of other samples with closely related concentrations and thicknesses showed similar results. The lh-hh (light-hole–heavy-hole) splitting in this sample was < 1 meV indicating that the layer can be regarded as almost unstrained. In Fig. 1 typical Raman spectra are plotted for $B = 6$ T with an excitation energy close to the spin split excitonic transitions at the E_0 gap. With polarizations of incident and scattered light parallel to each other [e.g., (π,π) geometry] longitudinal-optical (LO) phonon modes displaying the two-mode behavior of $Cd_{1-x}Mn_xTe$ are observed on a luminescence background. For (σ,π) geometry a strong additional line appears at 20.9 meV for $B = 6$ T overlapping with some of the weaker phonon structures (Fig. 1). This Raman excitation is strongly observed only in those scattering geometries that are allowed for SFRS. Its Stokes shift in a magnetic field (Fig. 2) shows a Brillouin-function-like behavior and agrees well with the spin spitting of the conduction band as it is measured, e.g., by PLE. In the following we therefore will promote the interpretation that the observed Raman signal results from the spin flip of an electron.

For vanishing external magnetic field there is a small residual spin splitting (see Fig. 2) that has been attributed to the formation of an *electron magnetic polaron*.[2–6,25,26] The magnetic polaron is a complex where the spin of a carrier and the localized magnetic moments of the Mn^{2+} *3d* states interacting with it tend to be aligned respective to each other. This results in a decrease of the total system energy and in a finite spin splitting of the electron states even at external field $B_{\mathrm{ext}} = 0$ T. The mean magnetic contribution to the localization energy of electrons is half the observed spin splitting at $B = 0$ T (~ 0.5 meV in Fig. 2). For comparison the much stronger Coulomb localization of an electron bound to a substitutional donor ion was measured in CdTe to be about 13.8 meV.[24] Thermodynamically at $T = 2\,\mathrm{K}$ an electron magnetic polaron should only be stable if the carrier is trapped by Coulomb interaction in addition to the rather weak magnetic localization.[25,26] The observation of a residual spin splitting at $B = 0\,\mathrm{T}$ displaying magnetic polaron formation therefore indicates that the electron changing its spin should be trapped mainly by Coulomb interaction, i.e., at a donor.

The magnetic field dependence of the full width at half maximum (FWHM) of the Raman line under discussion is shown in Fig. 3. For a Raman shift larger than 8 meV (magnetic field $B > 1\,\mathrm{T}$, see Fig. 2) the FWHM is proportional to the spin splitting. This can be explained, first, by alloy fluctuations resulting in variations of the total number of Mn spins interacting with the electrons

bound on the spatially distributed donors and, second, by the spatial variations of the antiferromagnetic coupling between these Mn spins. The spin relaxation time should not significantly affect the FWHM of the Raman excitation. This can be concluded from SFRS on free electrons,[9] where the spin relaxation time is mainly determined by scattering at local variations of the magnetization or by scattering at nonmagnetic impurities. Both relaxation channels do not hold for bound carriers. For $B < 1$ T an additional contribution to the FWHM is observed in Fig. 3. It is due to the temporal fluctuations of the Mn spin orientations within an electron bound magnetic polaron. This contribution to the FWHM is another indication for magnetic polaron formation and therefore again confirms the bound state of the electron, which changes its spin.

The spin splitting of the *valence-band states* in $Cd_{1-x}Mn_xTe$ is well known to be 33% larger than that of the conduction band.[23] From a comparison between

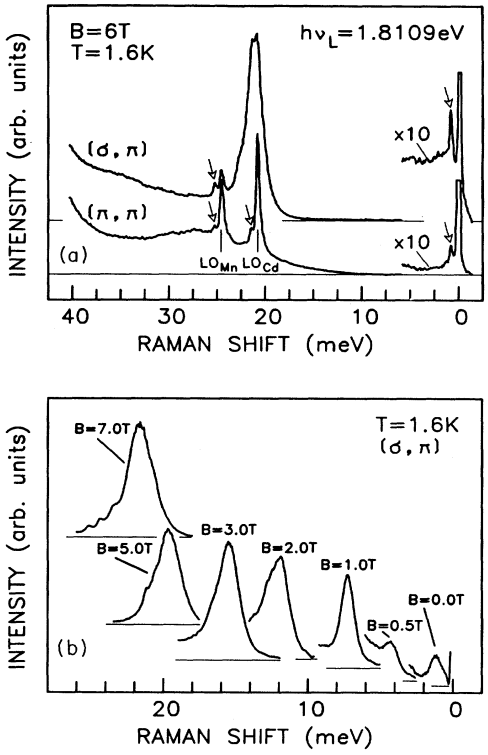

FIG. 1. (a) (σ,π) and (π,σ) Raman spectra of a $Cd_{0.865}Mn_{0.135}Te$ epilayer (thickness 1.6 μm) at $B = 6$ T and $T = 1.6$ K with excitation ($h\nu_L = 1.8109$ eV) in the energy range of the spin-split excitonic transitions. The baseline of the upper spectrum is shifted for clarity. The increase of the background with photon energies < 1.78 eV is due to the onset of the intensive $1(\sigma)$ band-edge luminescence (for the notation see Fig. 5), which is displayed in Fig. 6. The (π,π) spectrum shows the two LO phonon modes and a weak luminescence background centered at 1.785 eV, which is due to the recombination of not yet thermalized $2(\pi)$ lh excitons. In the (σ,π) polarized spectrum an additional excitation corresponding to the spin-flip of electrons appears at 20.9 meV. Phonons as well as the Rayleigh scattered laser light show 0.7-meV Stokes shifted sidebands marked by arrows. They display spin-flip Raman transitions in the Zeeman split $^6S_{5/2}$ ground state of the *3d* shell in Mn^{2+} respective combination processes of this spin-flip and the creation of a phonon (Ref. 34). The appearance of this *3d* excitation in the SFRS forbidden (π,π) geometry can be attributed to double resonance effects (Ref. 14). (b) Spin-flip Raman spectra of this $Cd_{0.865}Mn_{0.135}Te$ sample at different magnetic fields in (σ,π) polarization. All spectra were taken in resonance with the energy of the spin split exciton. The spectrum at $B = 0$ T proves the existence of an electron bound magnetic polaron (Ref. 26).

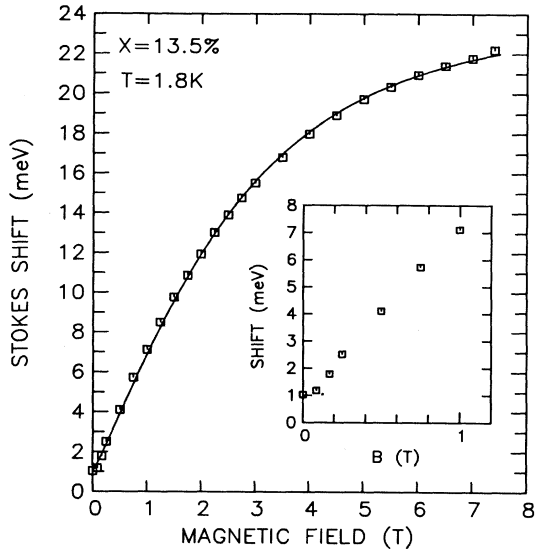

FIG. 2. Stokes shift of the SFRS line shown in Fig. 1 vs magnetic field. At $B = 0$ T a small residual Raman shift (about 1 meV, see inset) is due to the spin splitting of the electron states in an electron magnetic polaron. The solid line is a fit using the formula of Peterson *et al.* (Ref. 6) considering the Brillouin-function-like spin splitting of the electron states as well as the small effect of the bound magnetic polaron (Ref. 26) at $B = 0$ T.

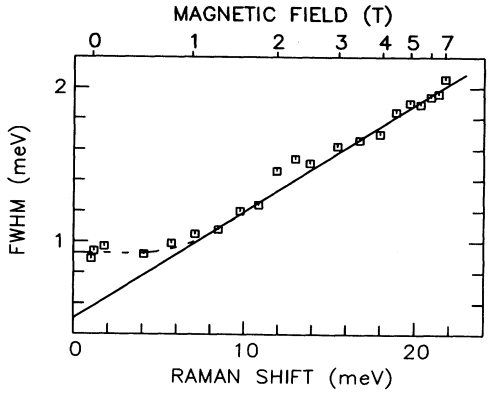

FIG. 3. FWHM of the spin-flip Raman excitation as a function of the spin splitting (Raman shift), $T = 1.8$ K; x=13.5%. The spectral resolution of the spectrometer was 0.4 meV.

the observed Raman shift and the PLE transitions one therefore can exclude the spin-flip of a *free hole* to be responsible for the observed SFRS excitation. However the spin splitting of the $j = 3/2$ ground state of a *hole bound to an acceptor* can be rather different and was calculated to be nonequidistant.[27,28] Unfortunately so far no experimental observation of the spin splitting in the acceptor ground-state multiplet is available for semimagnetic semiconductors. Due to the large splittings in these materials only the lowest spin component $m_j = -3/2$ should be occupied at 1.6 K. In the (σ, π) scattering geometry used for the upper spectrum of Fig. 1 one expects to observe Raman transitions with $\triangle m_j = +1$, i.e., from the $m_j = -3/2$ to $m_j = -1/2$ component in the acceptor ground-state multiplet. Especially this spin splitting between the states $m_j = -3/2$ and $m_j = -1/2$ has been calculated to be significantly smaller than for free holes and to be about the splitting of the conduction band. So from the observed Raman shift alone one cannot exclude observing SFRS on acceptor bound holes.

In contrast to the spin splittings at finite magnetic fields the magnetic polaron effect at $B_{\text{ext}} = 0$ T is expected to be completely different for bound electrons and bound holes and therefore can be used to distinguish between them: The lowest spin component $m_j = -3/2$ of the acceptor ground state can be measured by the electron acceptor transition in photoluminescence. At $B_{\text{ext}} = 0$ T one observes a well-known magnetic contribution to the binding energy of the hole at the acceptor which is attributed to the formation of a magnetic polaron complex around the bound hole.[29–31] This magnetic contribution to the localization energy can be regarded as the effect of the large internal magnetic field within an acceptor bound magnetic polaron although the external field is zero. The magnetic localization energy increases with the concentration x of the Mn^{2+} ions and reaches a maximum of 45 meV at $x = 0.25$ ($T = 5$ K).[30] For $x = 0.135$ one expects an internal magnetic field of the order of $B_{\text{int}} = 10$ T (see Ref. 30). One therefrom estimates the $m_j = -3/2$ to $m_j = -1/2$ SFRS transition of the hole involved to be about 23 meV. This is more than one order of magnitude larger than the electron splitting observed in Fig. 1 for $B_{\text{ext}} = 0$ T. We therefore conclude that in the samples under investigation the carrier which changes its spin cannot be a bound hole. In addition, the interpretation as SFRS on a donor bound electron is confirmed by the resonance behavior of the SFRS signal which is discussed Sec. III B.

To probe the excitation channel of the donor bound electrons we have investigated the SFRS efficiency I_{SFRS}/P_L as a function of incident laser power P_L at $B = 6$ T (Fig. 4). The SFRS efficiency in our n-type sample is found to be independent of the photon density; therefore the Raman signal cannot be a consequence of photon-created electrons. This agrees well with what is

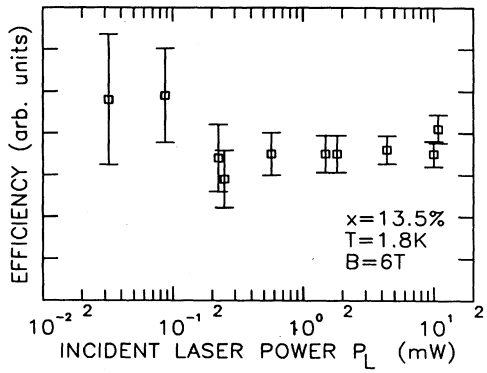

FIG. 4. SFRS efficiency I_{SFRS}/P_L as a function of intensity I_{SFRS} and the incident laser power P_L for a $Cd_{0.865}Mn_{0.135}Te$ epilayer grown by photoassisted MBE. A laser power of 1 mW incident into the cryostat corresponds to a power density of 0.16 W cm^{-2} at the sample surface. Large error bars at low power densities result from the low signal intensity. For $P_L > 0.5$ W cm^{-2} the Brillouin-function-like spin splitting and thus the resonance profile for SFRS was observed to shift slightly (< 0.3 meV) as a consequence of sample heating. The data were taken exactly at the maximum of the resonance profile (FWHM $\Gamma = 9$ meV, Fig. 6) to make sure that the observed lowering of the spin splitting by temperature does not significantly affect the measured scattering efficiency.

expected from the photoassisted MBE growth process. The substitutional as well as possible intrinsic donor impurities should be activated by the photoassisted MBE process. Recently Gubarev, Ruf, and Cardona[20] investigated a p-type $Cd_{0.95}Mn_{0.05}Te$ bulk sample ($N_A - N_D = 5 \times 10^{16}$ cm^{-3}). They observed a similar spin-flip excitation and assigned it to the spin-flip of photoexcited electrons trapped at ionized donors. According to that they found a nonconstant behavior of the SFRS efficiency at low power densities (in contrast to the results of the n-type sample shown in Fig. 4) and a saturation behavior at higher power densities, where all thermally ionized donor atoms have then trapped a photocreated electron.

B. Scattering process

A schematic representation of the spin splittings in the Γ_8 valence- and Γ_6 conduction-band states is shown in Fig. 5. Dipole transitions, which are allowed in Voigt geometry, are labeled by numbers 1–6 and characterized by their polarizations σ and π. For SFRS on a carrier one expects a scattering process that can be written in second-order perturbation theory. If the carrier is bound and the concentration of the donors is reasonable low, dispersion can be neglected and one deals with the scattering probability for a single atom,[32]

$$\frac{d\sigma}{d\omega} \propto \left| \frac{1}{m^2} \sum_l \left\{ \frac{\langle f|\mathbf{e}_S^* \cdot \mathbf{D}|l\rangle\langle l|\mathbf{e}_I \cdot \mathbf{D}|i\rangle}{E_i + \hbar\omega_I - E_l} + \frac{\langle f|\mathbf{e}_I \cdot \mathbf{D}|l\rangle\langle l|\mathbf{e}_S^* \cdot \mathbf{D}|i\rangle}{E_i - \hbar\omega_I - E_l} \right\} \right|^2 . \quad (1)$$

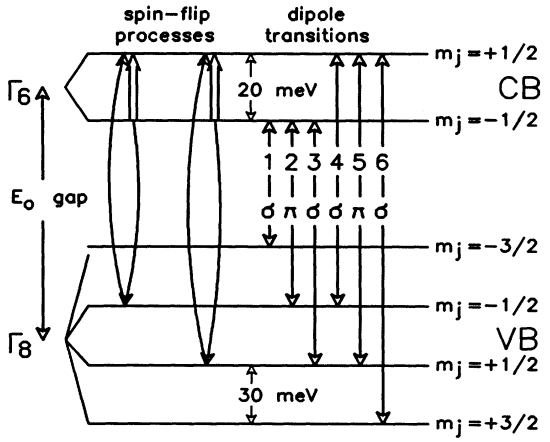

FIG. 5. Schematic representation of the spin splittings for Γ_8 valence- and Γ_6 conduction-band states. The dipole transitions, which are allowed in Voigt configuration, are numbered 1–6 and characterized by their polarizations. For $B = 6$ T, $T = 1.8$ K, and a Mn concentration of 13.5% (as realized in the sample discussed in the text) the symmetric splittings of valence and conduction band are about 30 meV and 20 meV, respectively. On the left side of the diagram the two Raman processes contributing to the SFRS on Γ_6 electrons are shown schematically.

Here $\mathbf{D}$ is the dipole operator, $\mathbf{e}_I$ and $\mathbf{e}_S$ are polarization vectors of incident and scattered waves, respectively. i, l, and f denote initial, intermediate, and final states of the process with their respective energies E_i, E_l, and E_f. Although the electric-field part of the electromagnetic wave interacts only with the orbital part of the states, the change of the spin is mediated by the spin-orbit interaction which mixes different spin contributions to the intermediate state l. For SFRS on conduction electrons therefore at least the Γ_8 and the spin-orbit split-off Γ_7 valence-band states have to be taken into account in the summation over l. Nevertheless, as the spin-orbit splitting is about 1.0 eV, only the denominators involving the Γ_8 valence-band states contribute significantly to resonance profiles obtained with excitation close to the band gap (one-level approximation). The dipole selection rules discussed in the Introduction allow SFRS in (σ,π) and (π,σ) geometry. Therefore scattering at the spin of a Γ_6 conduction electron ($j = 1/2$) is resonantly excited only via the $m_j = \pm 1/2$ ("light hole") valence-band components as intermediate states. The two resulting processes for Stokes scattering on Γ_6 electrons are shown on the left side of Fig. 5: The exciting photon creates an electron hole pair with the electron in the $m_j = +1/2$ excited spin state and the hole in one of the $m_j = \pm 1/2$ states, where the sign of the hole state depends on the scattering geometry. In the second step this hole recombines with an electron in the occupied $m_j = -1/2$ conduction-band state by emission of scattered light. The result is a spin-flip of an electron from $m_j = -1/2$ to $m_j = +1/2$ while the valence band is left unchanged. As energy conservation only holds for the whole scattering process, the scattered light is Stokes shifted by the spin splitting of the electron states for any exciting laser energy. Due to the resonance denominators one can expect maximum scattering probability, if the energy of the laser photon is equal to the $4(\sigma)$ or the $5(\pi)$ transition (Fig. 5) depending on the geometry. At resonance the energy of the scattered light then has to be equal to the $2(\pi)$ or the $3(\sigma)$ transition, respectively.

Figure 6 shows in its upper part the scattering efficiency of the SFRS excitation plotted as a function of the energy of scattered light. A very clear resonance is observed in both scattering geometries. To characterize the dipole transitions involved, the lower parts in Fig. 6 display luminescence and PLE spectra measured at the same magnetic field and temperature. The distinct features in the PLE spectra are attributed to the creation of free excitons and correspond to the $1(\sigma)$ and $2(\pi)$ transitions in Fig. 5. In agreement with the dipole selection rules resonance for the SFRS is observed, if the energy of the scattered light is equal to the transitions $2(\pi)$ and $3(\sigma)$. The exciton binding energy in CdTe is 10 meV.[28] This value should only weakly depend on Mn concentration, because the band-edge parameters depend only slightly on x. So transitions between states of free particles can be expected to be clearly separable from the re-

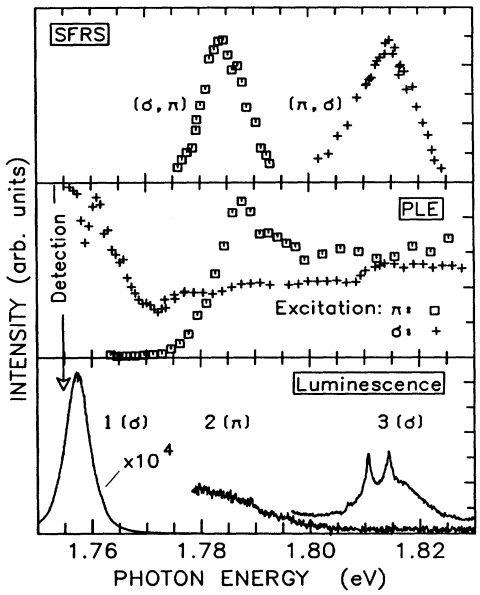

FIG. 6. Luminescence, PLE, and SFRS efficiency as a function of the quantum energy of scattered (exciting) light for a $Cd_{0.865}Mn_{0.135}Te$ epilayer at $B = 6$ T and $T = 1.8$ K plotted on the same energy scale. Luminescence shows recombination of $1(\sigma)$ ("heavy hole") excitons as well as much weaker recombination of not yet thermalized $2(\pi)$ and $3(\sigma)$ ("light hole") excitons (see Fig. 5). The σ and π PLE spectra were recorded with detection on the $1(\sigma)$ luminescence and display distinct features, which correspond to the lowest σ and π exciton transitions, respectively, as well as broader structures which result from higher energy transitions. SFRS shows resonance if the energy of the scattered light is equal to the $2(\pi)$ or the $3(\sigma)$ excitonic transition respective to the scattering geometry.

spective excitonic transitions. From the good agreement between the position of the excitonic resonance maxima in PLE and of the resonance for SFRS efficiency (Fig. 6) we therefore conclude that excitons serve as intermediate states of the SFRS process.

We have to emphasize that the two resonances of SFRS shown in Fig. 6 cannot be described by scattering on thermalized holes: According to dipole selection rules Raman scattering, where a hole changes its spin by $\triangle m_j = +1$, is expected to show two resonances at the E_0 gap in (π, σ) as well as two in (σ, π) scattering geometry. Which of the four processes contributes to SFRS depends not only on the geometry but also on the spin of the hole in the initial state. If the (free or bound) hole is thermalized in a $m_j = -3/2$ state, only one resonance for a $m_j = +1$ scattering process is expected in (π, σ) geometry with an energy of the scattered photon close to the $1(\sigma)$ exciton transition. No resonance of the spin-flip excitation under discussion has been observed however for this energy. On the other hand, if such a resonance is less developed than the two resonances shown in Fig. 6, it probably is difficult to observe as the intense $1(\sigma)$ luminescence background covers this transition. Finally—according to the selection rules used—the resonances shown in Fig. 6 also could be due to scattering on not yet thermalized holes in the $m_j = +1/2$ and $m_j = -1/2$ states, respectively. Nevertheless it seems unlikely that strong SFRS on excited but not on thermalized holes should be observed.

In the case of SFRS on donor bound electrons the photoexcited exciton with electron spin $m_j = +1/2$ is instantaneously interacting with the $m_j = -1/2$ donor electron. This intermediate state of the SFRS process therefore should be a *donor bound exciton* (D^0, X), i.e., a localized excited state of the neutral donor complex. The (D^0, X) involved in SFRS can be considered as a diatomic-molecule-like system with the donor and the exciton's hole component as heavy nuclei, while the binding between them arises from two s-like electrons in a singlet state. From this model one can expect the resonance of the scattering process to be Stokes shifted relatively to the free exciton transition by the binding energy of this pseudomolecule, i.e., the localization energy of the exciton at the donor. For CdTe the localization energy of excitons at substitutional donors (e.g. Ga, In, Cl) is known from luminescence to be 3.3–3.6 meV depending only slightly on the type of the donor.[24] The Voigt geometry allows a very precise determination of the $2(\pi)$ "light-hole" free exciton transition, e.g., by PLE (see Fig. 6). In addition the resonances of the SFRS are rather distinct due to the antisymmetric character of the Raman scattering on a magnetic dipole.[15] This enables us to perform a very accurate comparison between the energy of the $2(\pi)$ free exciton transition and the resonance energy of SFRS in (σ, π) geometry. Figure 7 shows that the Raman resonance is Stokes shifted relative to the free exciton transition by 3–4 meV in good agreement with the localization energy of an exciton at a substitutional neutral donor.

It has to be emphasized that the intermediate (D^0, X) involved in this scattering process is different from the thermalized (D^0, X) observed in luminescence experiments: In the case of the SFRS on a donor bound electron the $m_j = \pm 1/2$ hole component involved in the intermediate (D^0, X) complex is in an excited spin state and one deals with a not yet thermalized "hot" exciton. Nevertheless this exciton is a localized excited state of the neutral donor. In a semimagnetic semiconductor the (D^0, X) complex displayed by luminescence also has been observed to become unstable with increasing magnetic field and to dissociate into a neutral donor and a *free* exciton.[33] This corresponds to the fact that in a semimagnetic material even at moderate magnetic fields of about $B = 1\,\mathrm{T}$ the sum of the energies of a neutral donor and of a *free* exciton both with their electrons in the energetically lower spin state can be smaller than the energy of the (D^0, X) system. If the field is further increased one also expects one of the three excited triplet states of the (D^0, X) to become energetically lower than the singlet state. Nevertheless as a consequence of the Raman selection rules the SFRS resonance displays the (D^0, X) singlet state involving a "light"-hole component unaffected by the fact that energetically lower states of the complex may exist. Due to the very fast time scale of the scattering process it does not matter if the intermediate state is thermodynamically unstable.

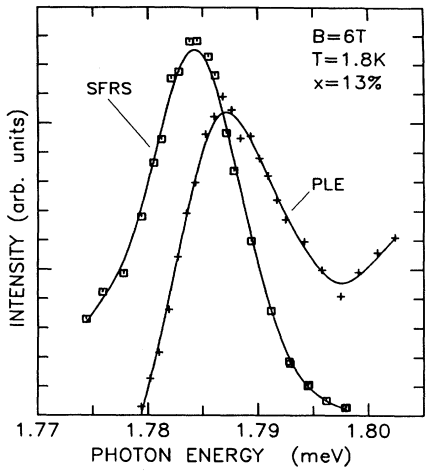

FIG. 7. Intensity of the SFRS in (σ, π) geometry as a function of scattered photon energy (squares) and PLE structure (crosses) of the free exciton absorption at the $2(\pi)$ transition. For the PLE spectrum a background of 10 units has been subtracted for clarity. SFRS shows resonance if the energy of the scattered photon is 3–4 meV Stokes shifted relative to the PLE free exciton structure.

If the external magnetic field is altered, the energy of the (D^0, X) singlet is changed corresponding to the Zeeman effect of the hole involved. However, as the two electrons in the singlet state should be responsible for the interaction between neutral donor and exciton, the localization energy itself is expected to be unaffected by a magnetic field. The Stokes shift between π PLE and (σ, π) SFRS resonance is in fact found to be independent of the magnetic field (Fig. 8). In a reversed argumentation Fig. 8 shows how far the model of the (D^0, X) as a pseudodiatomic molecule can be used: Although in the

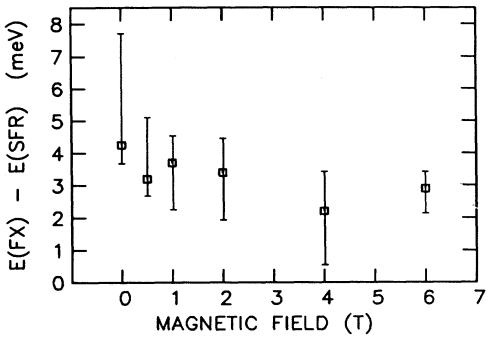

FIG. 8. Energy difference (Stokes shift) between the 2π free exciton structure displayed by PLE and the resonance of SFRS in (σ,π) geometry (Fig. 7). The shift is found to be independent of the magnetic field.

(D^0,X) the second "nucleus" is a hole with a $m_j = \pm 1/2$ angular momentum, the exchange interaction responsible for the localization is obviously not affected essentially by the magnetic field as it is mainly due to the electron singlet.

As the SFRS observed can be attributed to bound states, the linewidths of the resonance profiles display the lifetime of the states involved in addition to a Gaussian broadening due to the alloy fluctuations. In the samples under investigation the SFRS resonances of the energetically higher (π,σ) process are systematically broadened compared to the (σ,π) process (Fig. 6). The same broadening of resonance profiles with increasing transition energy has been observed for the resonances of SFRS on the Zeeman split Mn *3d* in its ground state[21] as well as for the resonances of Raman scattering on LO phonons in $Cd_{1-x}Mn_xTe$ bulk samples.[17] This tendency is also observed as a systematic increase in linewidth of the PLE free exciton structure with increasing transition energy [see, e.g., transition $1(\sigma)$ to $2(\pi)$ in Fig. 6]. We attribute the additional broadening of excitonic transitions with higher energy to a drastic decrease in the lifetime of the excited exciton transitions. A rough estimate leads to lifetimes in the picosecond range. We suggest that this very rapid decay of excited spin states is due to the strong exchange coupling in semimagnetic materials, which allows a very fast spin transfer to the Mn *3d* states. The residual Gaussian contribution to the linewidth of the excitonic transitions displayed by SFRS and PLE can be well understood in terms of the alloy broadening for the corresponding concentrations (see, e.g., Ref. 17).

IV. CONCLUSION

We have performed a study of the SFRS on electrons in bulklike semimagnetic $Cd_{1-x}Mn_xTe$:In epilayers. Stokes shift, the observation of a small magnetic polaron effect for vanishing magnetic field as well as the energetic position of the two resonances observed in $\bar{z}(\sigma,\pi)z$ and in $\bar{z}(\pi,\sigma)z$ scattering geometry indicate that a donor bound electron changes its spin. For the $\bar{z}(\sigma,\pi)z$ scattering geometry a very accurate comparison can be made between the energy of the free exciton displayed by PLE and the energy of the resonant intermediate state in SFRS. We therefrom conclude that a donor bound exciton (D^0,X) serves as intermediate state in this Raman process. Due to its very fast time scale the scattering is unaffected by the fact that the state of the (D^0,X) involved may be thermodynamically unstable. For the widely studied resonance behavior of Raman scattering on phonons it has been shown that excitonic states have to be taken into account for a better understanding of the observed resonance profiles (see, e.g, Ref. 17 and references therein). Our results about the SFRS on donor bound electrons as well as our studies about the SFRS on the Zeeman split *3d* groundstate of the Mn^{2+} ions[21] emphasize the importance of excitons also for the spin-flip Raman scattering process.

ACKNOWLEDGMENTS

We thank Professor Dr. G. Schaack and Dr. J. Kraus (Würzburg) for their support and critical reading of the manuscript. We also wish to acknowledge helpful discussions with Dr. S. I. Gubarev (Chernogolovka) and Professor Dr. O. Goede (Berlin).

[1]For a review see, e.g., O. Goede and W. Heimbrodt, Phys. Status Solidi B **146**, 11 (1988).
[2]N. Nawrocki, R. Planel, G. Fishman, and R. R. Galazka, Phys. Rev. Lett. **46**, 735 (1981).
[3]D. L. Peterson, A. Petrou, M. Dutta, A. K. Ramdas, and S. Rodriguez, Solid State Commun. **43**, 667 (1982).
[4]D. Heiman, P. A. Wolff, and J. Warnock, Phys. Rev. B **23**, 4848 (1983).
[5]D. L. Alov, S. I. Gubarev, and V. B. Timofeev, Zh. Eksp. Teor. Fiz. **84**, 1806 (1983) [Sov. Phys. JETP **57**, 1052 (1983)].
[6]D. L. Peterson, D. U. Bartholomew, U. Debska, A. K. Ramdas, and S. Rodriguez, Phys. Rev. B **32**, 323 (1985).
[7]E.-K. Suh, D. U. Bartholomew, A. K. Ramdas, R. N. Bicknell, R. L. Harper, N. C. Giles, and J. F. Schetzina, Phys. Rev. B **36**, 9358 (1987).
[8]D. L. Alov, S. I. Gubarev, and V. B. Timoveev, Zh. Eksp. Teor. Fiz. **86**, 1124 (1984) [Sov. Phys. JETP **59**, 658 (1984)].
[9]T. Dietl, M. Sawicki, M. Dahl, D. Heiman, E. D. Isaacs, M. J. Graf, S. I. Gubarev, and D. L. Alov, Phys. Rev. B **36**, 9358 (1991).
[10]D. Heiman, A. Petrou, S. H. Bloom, Y. Shapira, E. D. Isaacs, and W. Giriat, Phys. Rev. Lett. **60**, 1876 (1988).
[11]D. Scalbert, J. Cernogora, A. Mauger, C. Benoit à Guillaume, and A. Mycielski, Solid State Commun. **69**, 453 (1989).
[12]D. Scalbert, J. A. Gaj, A. Mauger, J. Cernogora, and C. Benoit à Guillaume, Phys. Rev. Lett. **62**, 2865 (1989).
[13]A. Twardowski, D. Heiman, Y. Shapira, T. Q. Vu, and M. Demianiuk, Solid State Commun. **82**, 229 (1992).
[14]R. Meyer, J. Stühler, and G. Schaack (unpublished).

[15]G. Abstreiter, M. Cardona, and A. Pinczuk, in *Light Scattering by Free Carrier Excitations in Semiconductors*, edited by M. Cardona and G. Güntherodt, Topics in Applied Physics Vol. 54 (Springer-Verlag, Berlin, 1984).

[16]See, e.g., S. R. J. Brueck, A. Mooradian, and F. A. Blum, Phys. Rev. B **7**, 5253 (1973). Resonant spin-flip Raman scattering in GaAs/$Ga_{1-x}Al_xAs$ quantum-well structures has been reported by V. F. Sapega, M. Cardona, K. Ploog, E. L. Ivchenko and D. N. Mirlin, *ibid.* **45**, 4320 (1992).

[17]E. F. Schubert, E. O. Göbel, Y. Horikoshi, K. Ploog, and H. J. Queisser, Phys. Rev. B **30**, 952 (1980).

[18]S. I. Gubarev, T. Ruf, and M. Cardona, Phys. Rev. B **43**, 1551 (1991).

[19]R. Meyer, M. Hirsch, G. Schaack, A. Waag, and R.-N. Bicknell-Tassius, Superlatt. Microstruct. **9**, 165 (1991).

[20]S. I. Gubarev, T. Ruf, and M. Cardona, Phys. Rev. B **43**, 14 564 (1991).

[21]J. Stühler, M. Hirsch, G. Schaack, and A. Waag, in *Proceedings of the XIIIth International Conference on Raman Spectroscopy*, edited by W. Kiefer *et al.* (Wiley, Chichester, 1992), p. 862; (unpublished).

[22]A. Waag, Y. S. Wu, S. Schmeusser, M. Kraus, B. Schmied, W. Ossau, R. N. Bicknell-Tassius, and G. Landwehr, J. Cryst. Growth **117**, 820 (1992).

[23]J. A. Gaj, R. Planel, and G. Fishman, Solid State Commun. **29**, 435 (1979).

[24]Z. C. Feng, A. Mascarenhas, and W. J. Choyke, J. Lumin. **35**, 329 (1986).

[25]P. A. Wolff, *Semiconductors and Semimetals*, edited by R. K. Willardson and A. C. Beer (Academic, Boston, 1988), Vol. 25, p. 413.

[26]T. Dietl and J. Spalek, Phys. Rev. B **28**, 1548 (1983).

[27]L. R. Ram-Mohan and P. A. Wolff, Phys. Rev. B **38**, 1330 (1988).

[28]P. Janiszewski, *Proceedings of the 20th International Conference on the Physics of Semiconductors* (World Scientific, Singapore, 1990), p. 771.

[29]T. H. Nhung, R. Planel, C. Benoit à Guillaume, and A. K. Bhattacharjee, Phys. Rev. B **31**, 2388 (1985).

[30]M. Bugajski, P. Becla, P. A. Wolff, D. Heiman, and L. R. Ram-Mohan, Phys. Rev. B **38**, 10 512 (1988).

[31]M. Prakash, M Chandrasekhar, H. R. Chandrasekhar, I. Miotkowski, and A. K. Ramdas, in *Properties of II-VI Semiconductors: Bulk Crystals, Epitaxial Films, Quantum Well Structures, and Dilute Magnetic Systems,* edited by F. J. Bartoli, Jr., H. F. Schaake, and J. F. Schetzina, MRS Symposia Proceedings No. 161 (Materials Research Society, Pittsburgh, 1990), p. 449.

[32]See, e.g., W. Hayes and R. Loudon, *Scattering of Light by Crystals* (Wiley, New York, 1978).

[33]W. Heimbrodt, O. Goede, Th. Köpp, H.-G. Gumlich, H. Hoffmann, U. Stutenbäumer, B. Lunn, and D. E. Ashenford, *Proceedings of the 20th International Conference on the Physics of Semiconductors* (Ref. 28).

[34]A. Petrou, D. L. Peterson, S. Venugopalan, R. R. Galatzka, A. K. Ramdas, and S. Rodriguez, Phys. Rev. B **27**, 3471 (1983).